Summer Season Forecast Experiments with the NCEP Coupled Forecast System (CFS) Using Different Land Models and Different Initial Land States

Rongqian Yang, Ken Mitchell and Jesse Meng
Environmental Modeling Center, NOAA/National Weather Service

NOAA CTB - COLA
Joint Seminar
Mar. 26, 2008

ABSTRACT

It is well known that in the N.H. summer season, the ENSO signal and influence across the continental U.S.(CONUS) is much weaker than in the winter season, hence seasonal predictions by coupled global climate models manifest significantly lower skill over CONUS in the summer than in the winter season. Research over the past decade has demonstrated that proper land state initialization (especially soil moisture) can be important to global model seasonal predictions for summer precipitation over CONUS. In this study, we use the state-of-the-art NCEP Coupled Forecast System (CFS) to examine the extent to which upgrades to the land model and land data assimilation component of the CFS can improve CFS summer season predictions over the CONUS.

The CFS, which is equipped with the modern Noah Land Surface Model (Noah LSM), is initialized with three different initial land states (GR2, GLDAS, and GLDAS climo), in comparison with a CFS control run using the older OSU Land Surface Model (OSU LSM) with the GR2 initial land state. (Herein, "GR2" denotes the NCEP-DOE Global Reanalysis 2, which utilizes the OSU LSM, and "GLDAS" denotes the Global Land Data Assimilation System, which utilizes the Noah LSM.) CFS seasonal forecast experiments have been carried out for 25 different summers (1980-2004), each with 10 CFS ensemble members, whose initial starting dates are from April 19 to May 3. We examined the impact of two different land surface models and three choices of different initial land states on seasonal precipitation, 2-meter air temperature, 200 mb and 500 mb heights, SSTs, and on land surface fields including latent heat and sensible heat fluxes, among others. (Due to limitation of length of this report, we only present CFS summer seasonal precipitation performance, including one special case – a strong Southwest U.S. monsoon in summer 1999.)

Results from the CFS experiments indicate that achieving improvement in CFS performance from a land model upgrade requires the execution of a companion global land data assimilation system (GLDAS) with the very same new land model as utilized in the land-component upgrade of the global climate model. Providing the land surface model with compatible and self-consistent land states is important to seasonal predictions. In contrast, improper initialization of the land surface model can degrade the global model performance, suggesting it is naive to merely upgrade the land component of a global climate model for seasonal forecasting without simultaneously upgrading the land component of the companion global data assimilation system.

1. Introduction

The research literature has rather firmly established that large-scale anomalies in the atmospheric general circulation on seasonally-averaged time scales are forced first and foremost by large-scale anomalies in SST (especially in the tropical Pacific Ocean). Additionally, research has strongly indicated that the next most important forcing (albeit secondary to SST) of such anomalies is large-scale anomalies in the land states of soil moisture, snowpack, and vegetation cover [Koster et al. 2004]. The linkage between land surface anomalies and the spawning of seasonal atmospheric circulation anomalies has been harder to confirm and quantify than that of SST. Being a secondary forcing source to that of SST anomalies, land-anomaly forcing is more difficult to

Correspondence to: Ken Mitchell, NOAA/NWS/NCEP/Environmental Modeling Center
E-mail: Kenneth.Mitchell@noaa.gov

separate from the natural chaotic variability of seasonal circulations (i.e. land-anomaly impact has a smaller signal to noise ratio than SST impact). Therefore, harnessing the impact of land surface anomalies on seasonal prediction skill in operational practice, such as at NCEP, is a tremendous challenge that requires not only a large number of members in the ensemble set of seasonal predictions, but also special care in the treatment of land state initial conditions, especially root-zone soil moisture and seasonally persistent snow pack.

It is substantially more difficult to create global analyses of the initial land states from satellite and in situ observations than it is to apply satellite and in situ observations to create global analyses of initial SST state. For this reason, over the last three decades, global analyses of SST on say weekly intervals have been much more routinely available and sanctioned for use in global prediction models than the counterpart case for global soil moisture and snowpack analyses. During the past 8-10 years, a consensus is emerging [Dirmeyer et al. 1999; Mitchell et al. 2004; Rodell et al. 2004; Koster et al. 2004] that embraces the view that the best approach for providing global or continental-scale analyses of deep soil moisture and snowpack is to execute a continuously cycled, multi-year, global, uncoupled, temporal integration of a land surface model (LSM) forced by global analyses of observed atmospheric land surface forcing, especially global analyses of observed (non-model) precipitation and satellite observed (non-model) surface solar insolation. This approach is well illustrated in the Global Soil Wetness Project of the late 1990's [Dirmeyer et al. 1999]. Such approaches have become known as Land Data Assimilation Systems (LDAS), though many (not all) of these LDAS systems to date are so-called "open loop" systems that do not actually assimilate observations to directly update the land states, but rather let the LSM-simulated land states physically evolve freely in response to the external analyses of near-surface atmospheric forcing, especially precipitation analysis.

Additionally, it is now well established that the land surface model (LSM) component of any given global general circulation model (GCM) has its own inherent annual-cycle climatology of soil moisture (and snowpack at high latitudes) over each region of the global landmass. Moreover, this inherent LSM climatology can be quite different from one LSM to another [Dirmeyer et al. 2006; Koster and Milly 1997]. Therefore, the optimal land-state initial conditions for the LSM component of a given GCM should be generated by long-term multi-year (even multi-decade) executions of the given LSM in the LDAS mode described above. Long-term executions are essential to allow for the multi-year spin-up time scales of deep soil moisture.

The global Coupled Forecast System [Saha et al. 2006], or CFS, implemented by NCEP in 2004 represents NCEP's 2nd-generation seasonal forecast system, which is a global coupled atmosphere/ocean/land prediction system. Its development focused on upgrades to the ocean and atmospheric components and its Global Ocean Data Assimilation System (GODAS), but not land surface model upgrades. The currently operational CFS still executes the legacy Oregon State University (OSU) LSM (which is the old late 1980's ancestor of the Noah LSM) that was executed in NCEP's 1stgeneration seasonal forecast system.

There are two basic pathways for improving the representation of land surface processes in coupled global prediction models. One pathway is to advance the realism of the physical processes of the land surface component. A second pathway is to improve the specification of the initial conditions of the land states (e.g. soil moisture and snowpack) via global land data assimilation. In summary, the two pathways are:

- Improve and upgrade the physics of the LSM component of the GCM,
- Provide optimal initial conditions for the land states of the GCM's LSM component by executing the given LSM in global LDAS mode over multi-year periods.

To demonstrate the importance of each pathway, we proceed to improve the land representation in the global CFS along each of the two pathways. First off, we executed GLDAS to provide the CFS with optimal initial land states. Secondly, we employed the CFS to carry out a series of seasonal forecast experiments. The atmosphere component in these CFS experiments is taken from a recently operational version (August, 2007) of NCEP's global medium-range forecast system, known as the Global Forecast System (GFS) and the ocean model used in the CFS is GFDL MOM3. The CFS experiments are seasonal prediction experiments, in hindcast mode, described further next.

As described below, we set out to execute one set of seasonal prediction experiments for each of the two pathways above

1.1 Upgrade the LSM physics of the CFS

At NCEP, the Noah LSM was implemented in NCEP's operational GFS in late May 2005. Thus the Noah LSM is expected to be the land component of NCEP's next generation CFS for seasonal prediction. The current operational CFS at NCEP employs the OSU LSM, a respected but increasingly older and distance ancestor to the Noah LSM (see Table 1 for major differences between the two LSMs). The next generation CFS is anticipated to utilize the Noah LSM and execute at T126/L64 resolution. We employ the latter resolution in all CFS experiments here.

Noah LSM Features	OSU LSM Features
– 4 soil layers (10, 30, 60, 100 cm)	– 2 soil layers (10, 190 cm)
– frozen soil physics included	– no frozen soil physics
– surface fluxes weighted by snow cover fraction	– fluxes not weighted by snow fraction
– improved seasonal cycle of vegetation cover	– vegetation cover never less than 50%
– spatially varying root depth of 1-2 m	– spatially constant deep root depth of 2 m
– improved soil and snow thermal conductivity	– poor soil and snow thermal conductivity
– higher canopy resistance	– too low canopy resistance
– infiltration accounts for sub-grid variability in precipitation and soil moisture	– infiltration does not account for sub-grid variability in precipitation and soil moisture
– More	

Table 1 Characteristics of Noah LSM versus OSU LSM

1.2 Provide optimal land state initial conditions

As a prerequisite to the T126 resolution CFS experiments to be carried out, a GLDAS was constructed and executed over the 28-year period of 1979-2006 using the Noah LSM as the land model and on exactly the same computational native grid as that of the T126 CFS. In so doing, we took care to use exactly the same terrain field and land mask as in the T126 CFS, as well as all the same specifications of land surface characteristics (soil class, vegetation class, etc), land physical parameters, and same version of the Noah LSM (2.7.1) as employed in the CFS/Noah experiments. This T126 GLDAS/Noah suite provided both the instantaneous and climatological GLDAS/Noah land states used in the CFS Cases C and D (see below about CFS Experimental Design).

The precipitation forcing for the GLDAS/Noah executions is CPC's CMAP pentad analysis of observed precipitation, partitioned to 6-hourly amounts using the global precipitation fields of the NCEP-DOE Global Reanalysis 2 (GR2). Aside from the precipitation forcing, all remaining land-surface forcings for the GLDAS/Noah executions are taken from the GR2. This surface forcing is adjusted for the terrain height differences between the T62 GR2 and the T126 CFS using adjustment algorithms that have been extensively and widely applied in EMC's longstanding N. American Land Data Assimilation System [Mitchell et al. 2004]. Additional details and background of the NCEP-NASA Global Land Data Assimilation System (GLDAS) is given in [Rodell et al. 2004].

Here are the steps we followed:

- Execute the collaborative NCEP-NASA, uncoupled, land-only, open loop Global Land Data Assimilation System (GLDAS) with the Noah LSM on the computational grid of the T126 CFS.
- Use these GLDAS-Noah land states to provide the optimum land-state initial conditions for the Noah LSM component of the CFS-Noah runs in the CFS experiment below.

- Characterize and depict the global distribution and magnitude of the differences between the Noah-LSM consistent land-state database of these GLDAS-Noah runs and the land states from the NCEP coupled atmosphere/land Global Reanalysis 2 (GR2), which employed the older OSU LSM.
- Characterize and depict the differences in terms of both the respective land-state climatology of each system (GLDAS versus GR2) and the interannual variability of anomalies of each with respect to their own climatology. The uncoupled NASA-NCEP Global Land Data Assimilation System (GLDAS) covers over a 25-year hindcast period (1979-2004) on the T126 Gaussian grid of the next generation CFS. The physics, parameters, and configuration of the Noah LSM in the GLDAS will exactly match that of the Noah LSM component of the CFS. Additionally, the GLDAS/Noah configuration and its forcing sources will be such that future real-time GLDAS executions are feasible for initializing operational CFS real-time forecasts.

1.3 CFS experimental design

To demonstrate whether the replacement of the OSU LSM with the Noah LSM yields meaningfully significant improvement in CFS seasonal prediction skill and test the impact of different initial land states on summer season prediction, the T126 CFS was executed and assessed using the following 4 configurations for each summer of 1980-2004, each with 10 members (for which the initial dates are April 19-23 and April 29-May 3, all at the initial time of 00Z). The time and dates of the initial conditions follow those used in NCEP's presently existing hindcast database of the presently operational T62 CFS/OSU).

- A - CFS/OSU/GR2: - OSU LSM, Land ICs from GR2 (CONTROL)
- B - CFS/Noah/GR2: - Noah LSM, Land ICs from GR2
- C - CFS/Noah/GLDAS: - Noah LSM, Land ICs from GLDAS/Noah
- D - CFS/Noah/GLDAS-Climo: - Noah LSM, Land ICs from GLDAS/Noah climatology

For our control case we execute the T126 CFS with the older OSU LSM used in the present operational CFS and initialized in the old manner from the land states of the NCEP-DOE Global Reanalysis 2 (denoted GR2), as done in the present operational CFS. In addition to the control, we execute three CFS experimental configurations, altogether giving the above four CFS configurations. We hereafter denote these four CFS configurations as Cases A-D. For all 4 cases, the atmospheric initial conditions are from GR2 and the ocean initial conditions are from NCEP's MOM3-based Global Ocean Data Assimilation (GODAS).

In Case B, we replace the old OSU LSM with the Noah LSM, but still use the old source of initial land states, which is the old Global Reanalysis 2 (GR2) that includes the older OSU LSM in its assimilating global background model. In Case C, we not only replace the OSU LSM with Noah, but we also replace GR2 with the Noah-based GLDAS as the source of initial land states. Finally, in Case D, we replace the instantaneous initial land-states from GLDAS/Noah with the 28-year daily climatology of the GLDAS/Noah land states.

Here GLDAS/Noah denotes a 28-year retrospective execution of the GLDAS (described above in Section 1.2) with the same Noah LSM as used in the CFS experiments, and on exactly the same T126 native computational grid as the CFS runs, with the same terrain field, land mask, and specification of land surface characteristics as used with the Noah LSM in the CFS.

Prior to launching the experiments, the working hypothesis was that Case C would yield the most skillful forecast, because Case C makes use of both a more modern LSM (Noah LSM) and the self-consistent initial land states of the Noah-based GLDAS. Case D sets out to examine the impact of using GLDAS/Noah soil moisture climatology rather than instantaneous soil moisture states. Case B intends to illustrate what degradation in CFS performance is realized if we had not developed the GLDAS suite and had to resort to using the land states of the NCEP-DOE Global Reanalysis 2 (GR2), which is based on the older OSU LSM. Finally Case A (control) represents the situation wherein we assume that neither the Noah LSM nor the GLDAS/Noah had been developed and applied to the CFS.

For each of the four cases above, we executed ten members of 6-month CFS forecasts for each summer during the 25-year period of 1980-2004. Hence the total number of 6-month CFS hindcasts we executed was 1000 ($4 \times 10 \times 25$), which represents a huge undertaking in managing model runs and output files. The 10 members differ in the start date of their initial conditions from late April and early May. The ten initial start

dates for each of the 25 summers are Apr 19-23, Apr 29-30, and May 1-3. Late-April/early-May initial conditions were chosen because in operational practice at NCEP, the operational CFS members from initial dates around late April represent the most important ensemble set of CFS runs used operationally by CPC in formulating the mainline CPC summer forecast, which is issued in mid-May.

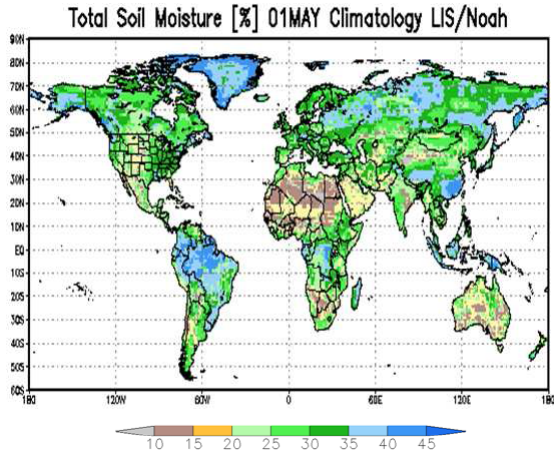

Figure 1 Climatology of total 2-m soil moisture (percent volumetric) of GLDAS/Noah on May 1.

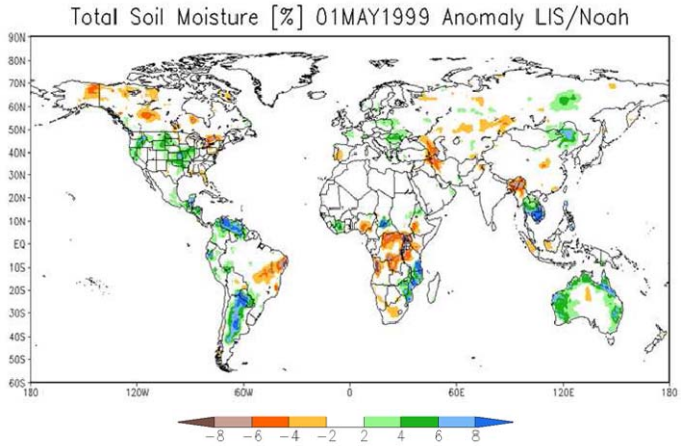

Figure 2 Anomaly of total 2-m soil moisture (percent volumetric) of GLDAS/Noah on May 1, 1999.

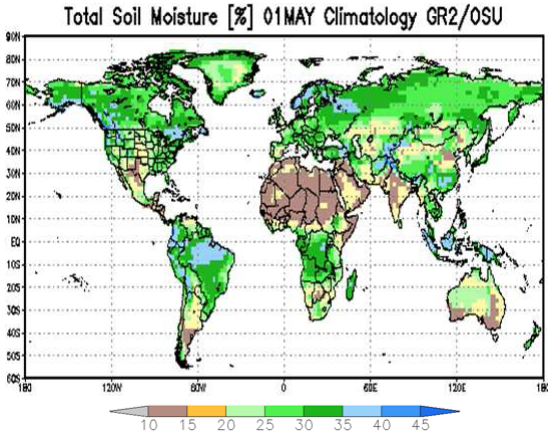

Figure 3 Climatology of total 2-m soil moisture (percent volumetric) of GR2/OSU on May 1.

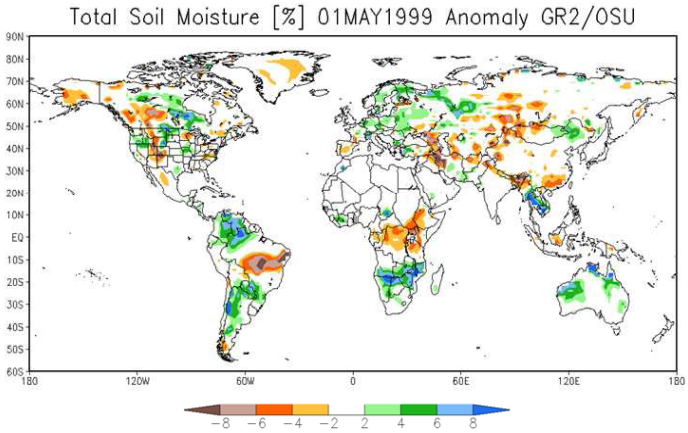

Figure 4 Anomaly of total 2-m soil moisture (percent volumetric) of GR2/OSU on May 1, 1999.

2. Results

2.1 The retrospective GLDAS for the CFS experiment and comparison with GR2

We first compare the land states of the 28-year retrospective T126 GLDAS/Noah, used in CFS cases C and D, with that of the NCEP/DOE Global Reanalysis 2 (GR2), used in CFS Cases A and B. The GR2 employed the older OSU LSM. Figure 1 and Figure 2, respectively, present global maps of the 01 May climatology and 01 May 1999 anomaly of the 2-meter soil moisture field from the GLDAS/Noah. Figures 3 and 4 are as in Figures 1 and 2, but from GR2/OSU. Figures 5-8 are as in Figures 1-4, but zoomed in over the CONUS domain. Both the GLDAS and GR2 simulate the soil moisture of a 2-meter soil column, albeit with four soil layers in GLDAS/Noah (0-10, 10-40,40-100, 100-200 cm) and only two layers in GR2/OSU (0-10, 10-190 cm). We choose to depict 01 May conditions, as that time is within the 19 April - 03 May period from which the initial conditions are taken for the 10 members of the summer CFS hindcasts. Comparison between the two sources of

soil moisture shows that the climatological values in early May of the GR2/OSU soil moisture are pervasively lower than those of GLDAS/Noah over the vast majority of both the global and CONUS domains (some exceptions).

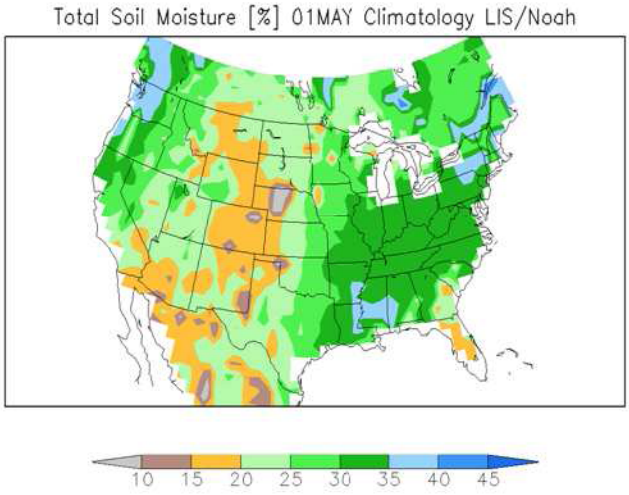

Figure 5 Climatology of total 2-m soil moisture (percent volumetric) over CONUS of GLDAS/Noah on Mav 1.

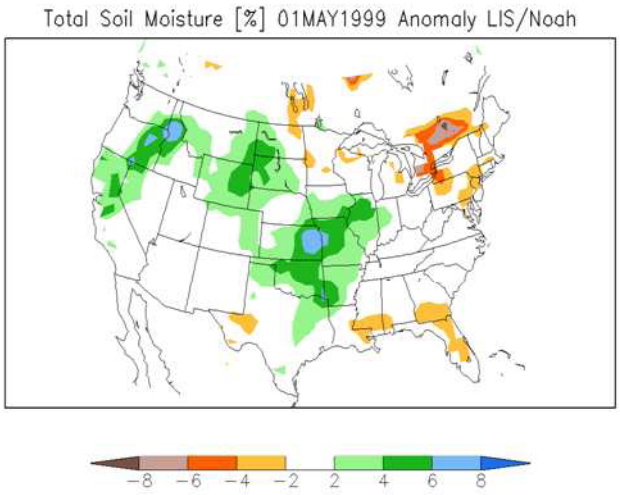

Figure 6 Anomaly of total 2-m soil moisture (percent volumetric) over CONUS of GLDAS/Noah on Mav 1. 1999.

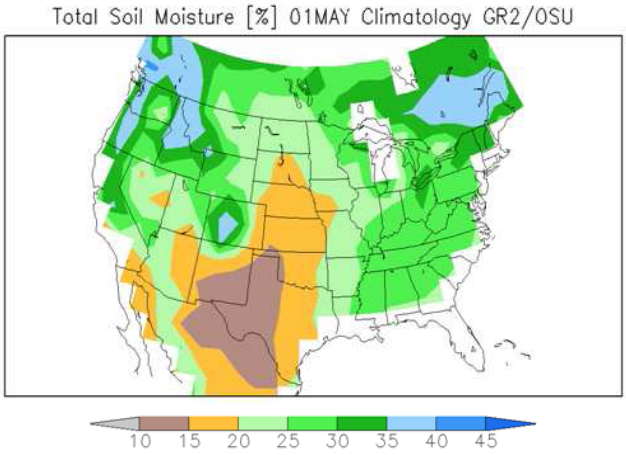

Figure 7 Climatology of total 2-m soil moisture (percent volumetric) over CONUS of GR2/OSU on May 1.

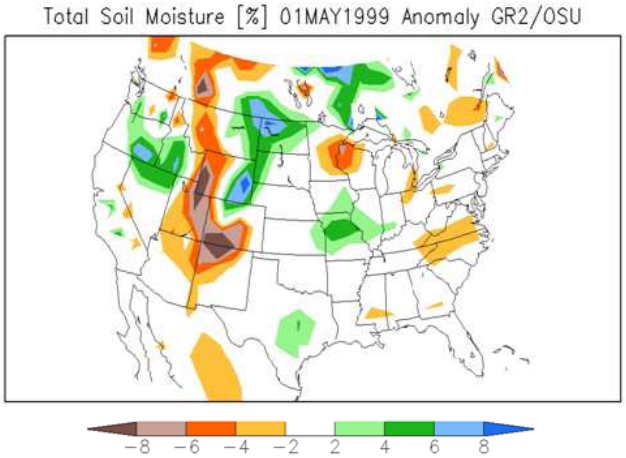

Figure 8 Anomaly of total 2-m soil moisture (percent volumetric) over CONUS of GR2/OSU on May 1, 1999.

The anomaly fields of GLDAS/Noah and GR2/OSU in Figures 2 and 4 show some similarities in some regions of the globe (S. America, Africa, Australia, Southeast Asia), but rather substantial differences over other regions (N. America and CONUS, southwest Asia, Europe). Focusing now on the latter substantial differences over CONUS, Figures 6 and 8 clearly reveal the large disagreement over CONUS between GLDAS/Noah and GR2/OSU soil moisture anomalies for the case of 01 May 1999. Figure 9 shows the observed precipitation anomaly for the 90-day period ending 30 April 99 (close in time to the 01 May 99 anomaly depicted in Figures 6 and 8). The GLDAS/Noah soil moisture anomaly in Figures 6 shows strikingly more spatial agreement with the observed precipitation anomaly than does GR2/OSU. This is because the GLDAS/Noah, unlike the GR2/OSU, uses an analysis of observed precipitation to force the land surface. To force its land surface, GR2/OSU uses the model precipitation from the background global model of the assimilation system. Over 5-day intervals, the GR2/OSU computes the errors in the model precipitation compared to the observed precipitation analysis (aside: the same precipitation analysis used directly by GLDAS above) and then subsequently applies a soil moisture

nudging scheme to try to offset the effects of the model's precipitation errors, but Figures 5-8 strongly suggests that the GR2/OSU nudging scheme is not effective.

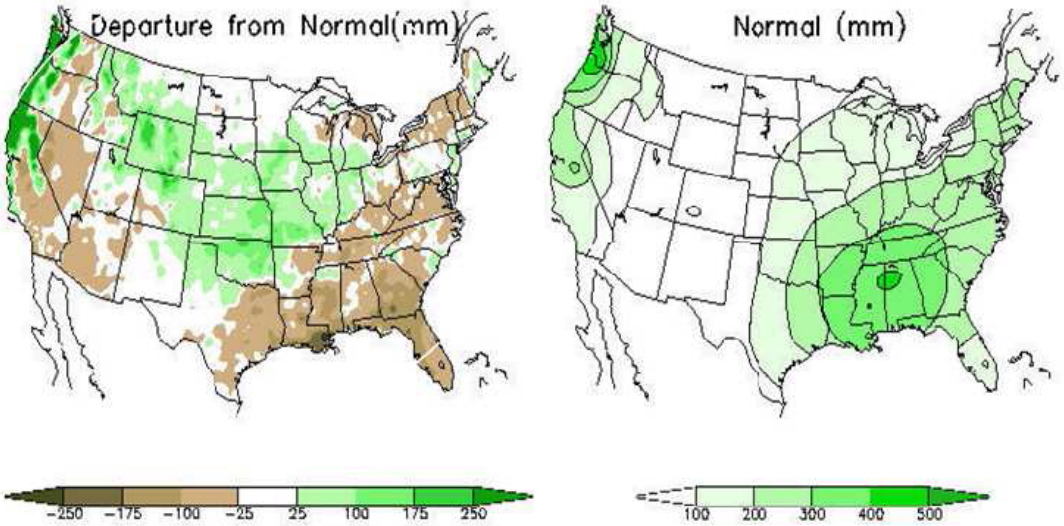

Figure 9 Observed 90-day of precipitation anomaly of 1999 (ended at April 30) (top) and climatology (bottom).

While Figures 1 to 8 are for a particular time of year, Figure 10 shows the multiyear time series and climatological annual cycle of monthly soil moisture (mm) from both the GLDAS/Noah and GR2/OSU for the 2-meter soil moisture (mm) spatially averaged over Illinois, plus the time series of the observed soil moisture derived from the Illinois network of soil moisture observations (Figure 9). Clearly in Figure 10, the soil moisture climatology of GR2/OSU remains consistently lower than that of GLDAS/Noah on a month-to-month basis year after year over the Illinois domain. Moreover in Figure 10, the higher GLDAS/Noah soil moisture is in closer agreement with the observations than that of GR2/OSU, though still exhibiting some low bias, but substantially less so than GR2/OSU.

One key implication to be drawn from Figure 10 and Figures 1 and 3 (climatology for 01 May from two sources of soil moisture) is that initializing the Noah LSM component of CFS from the notably drier states of the GR2/OSU soil moisture dataset will result in lower land surface evaporation in the CFS – a situation that is likely a significant contribution to the poor performance of the CFS/Noah/GR2 case (Case B) presented next in Section 2.2.

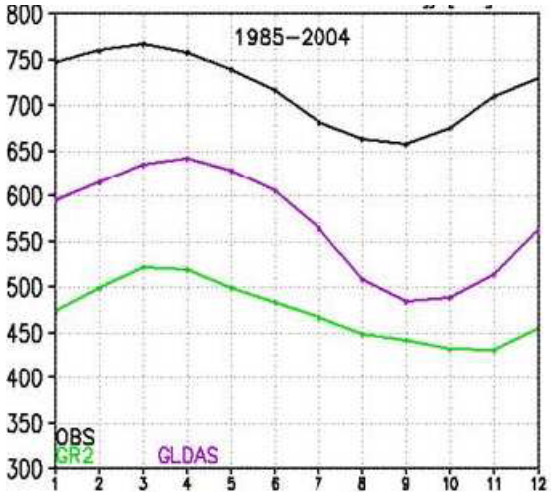

Figure 10 Climatology (1985-2004) of annual cycle of monthly 2-meter column soil moisture (mm) averaged over Illinois from GLDAS (purple), GR2 (green) and in situ observations (black).

2.2 CFS experiments results

It is known that seasonal prediction climate models have substantial systematic error. To overcome systematic error and achieve useful prediction skill, seasonal predictions from climate models are depicted as predicted anomalies from the model's own climatology. To derive the model climatology, it is necessary, as we do here, to execute a multi-decade ensemble-based reforecast of the climate model. Thus the first task after completing the 25-year summer-season reforecast set of 1000 members was to compute the CFS model climatology for each Case A-D.

The prior generation CFS manifested considerably useful

skill in predicting tropical Pacific SST (ENSO anomalies), but showed virtually no skill for predicting anomalies of summer precipitation total over CONUS. Therefore, we focus here on assessing Case A-D performance in predicting anomalies over CONUS of total 3-month precipitation for June-July-August (JJA). As our measure of CFS prediction skill for summer total precipitation, we will employ the primary CFS skill measure used by CPC, which is the anomaly correlation (AC) between CFS forecasts of precipitation anomalies and observed precipitation anomalies over the entire 25 years of the CFS reforecasts of Cases A-D. To defined the observed anomalies, we use the daily gauge-only 1/8th-deg CONUS precipitation analysis (with PRISM adjustment) produced by CPC for each day from 01 January 1979 to present. For application here, we spatially average this precipitation analysis to the T126 CFS grid (about 1-degree resolution) and compute the anomaly correlation (AC) score for precipitation on each CFS grid point over CONUS. This yields a CONUS map of AC score and this AC map is referred to as the CFS "skill mask".

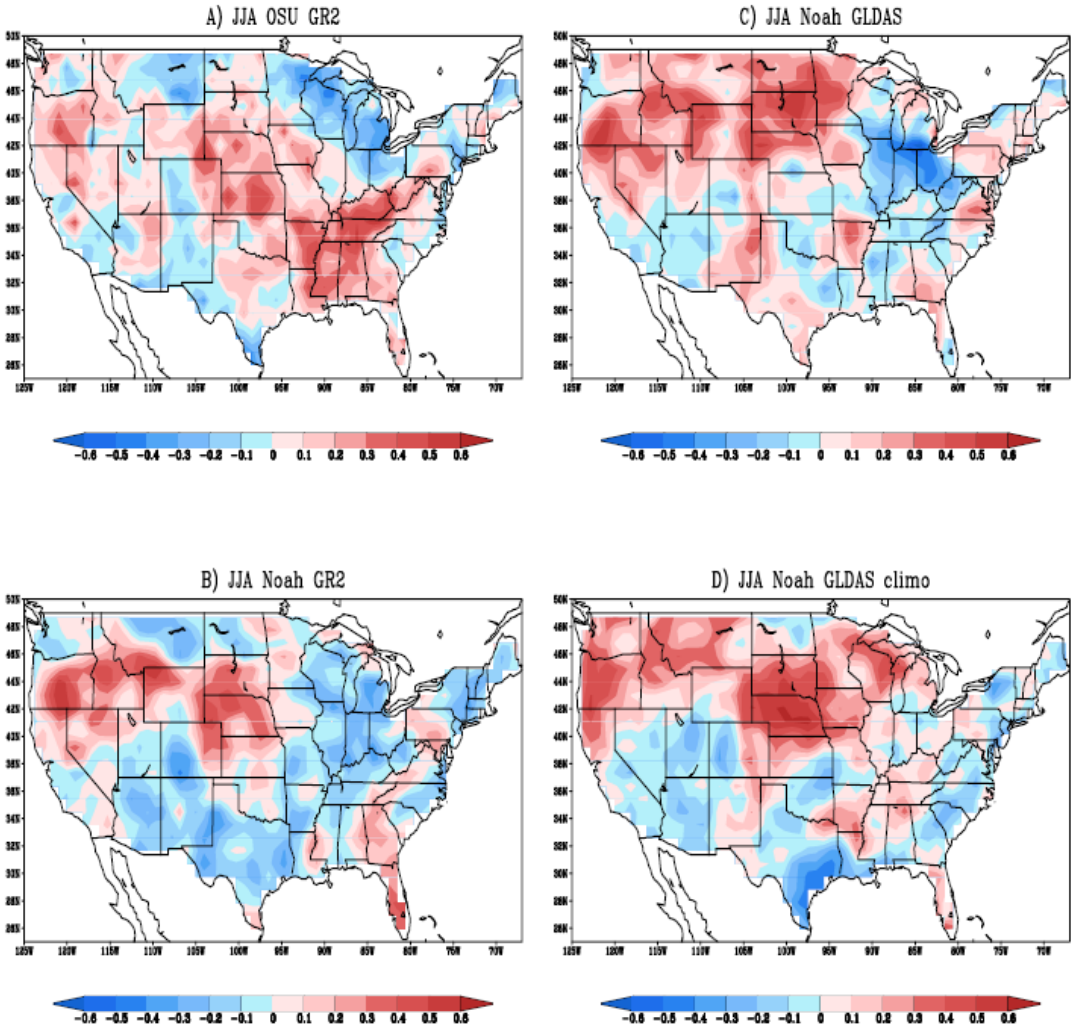

Figure 11 Anomaly correlation maps for 10-member ensemble mean seasonal forecasts of JJA precipitation from 25-year (1980-2004) reforecasts of four configurations of CFS using different land surface models and sources of initial land states. The ten members correspond to 10 different initial dates from 00Z of April 19-23 and April 30-May 3.

Here we present results from the extensive T126 CFS 25-year summer reforecast experiments of the four CFS configurations described above. The latter resolution of the new CFS is double the T62 resolution of the currently operational CFS. The CFS ocean model is the MOM-3 ocean model of GFDL. Specifically, the 10-

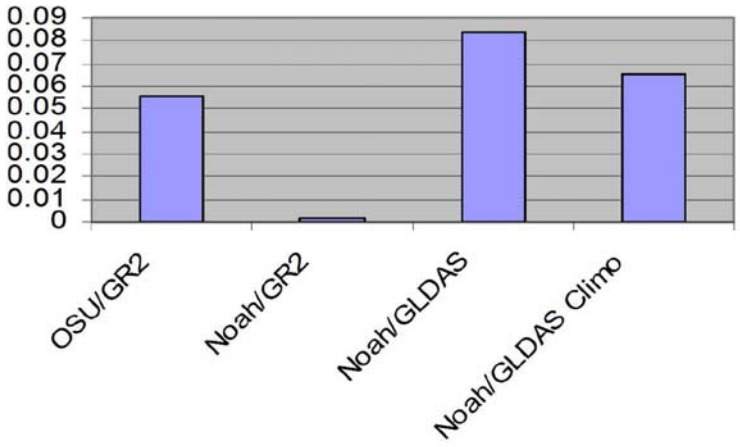

Figure 12 CONUS-wide spatial average anomaly correlation values from the four correlation maps presented in Figure 11.

member 6-month CFS reforecasts for each summer of the 25-year period of 1980-2004 were executed and assessed with four different land configurations (with and without the Noah LSM upgrade and with and without the Noah-based GLDAS) as described in Section 1.3. From the results of these experiments, we show below that the Noah LSM upgrade together with the Noah-based GLDAS improves the summer-season skill of CFS precipitation forecasts over the CONUS. The results illustrate that the Noah-based GLDAS is an important necessary component to realize the CFS forecast improvements from the Noah LSM upgrade.

The four panels of Figure 11 show the CONUS skill mask of AC score for JJA precipitation for each of the four CFS Cases A-D, as derived from the entire 25-year reforecast. The bar chart in Figure 12 shows the CONUS spatially averaged AC score. Figure 12 shows that Case C with both the Noah LSM upgrade and inclusion of the GLDAS/Noah does indeed yield the highest average AC score. Interestingly, Case D, which initializes the CFS Noah land states with the 25-year daily climatology of the 28-year GLDAS/Noah yields an AC score only modestly lower than that of Case C. Strikingly, and with far-reaching implications, Case B yields the lowest AC score by far (essentially zero). This result demonstrates that the real prediction benefit of upgrading the land model in a global model may likely not be realized if the global model is not provided with initial land states that are self-consistent with the inherent climatology and physics of the new land model. This strongly suggests that the global data assimilation system that is providing the initial land states for the global forecast model should be executing the same land model and same land surface characteristics and parameters as the global forecast model.

The spatial character of the AC skill masks of the four panels of Figure 11 are also very revealing. Case B is obviously far inferior to the other three cases. Also, each case yields different preferred regions for higher AC score, with Cases B-C showing a tendency to yield higher scores in the north central and northwest CONUS while Case A shows a different tendency toward higher scores in the south central and southeast CONUS. For Cases A and C only, an additional 5 members (15 members total) were executed and no appreciable difference in the spatial patterns of Figure 11 for those two cases was evident (not shown).

We emphasize that even though

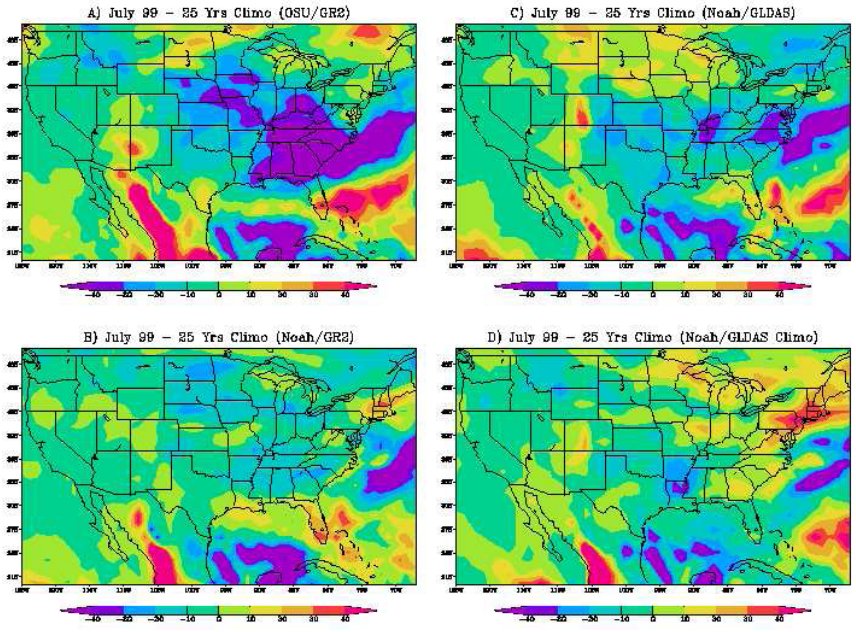

Figure 13 Ensemble mean CFS predicted precipitation anomaly (mm) for July 1999 from 10 CFS members of late April and early May initial conditions, using four different cases in CFS of choice of LSM and source of initial land states. The CFS anomalies are with respect to corresponding 25-year (1980-2004) reforecast climatology of each given CFS configuration.

Case C yields the highest AC score in Figure 12, even its value is distressingly low – of order 0.084 and hence not even reaching 0.1. Figure 11 reveals that even in the regions of positive AC values, the values usually do not exceed 0.4. Furthermore, even consistently predicting the correct sign of the anomaly over the entire CONUS remains illusive. Hence the seasonal prediction skill of summer precipitation over CONUS is still a major challenge, needing still much more effort (likely in CFS physics unrelated to the land surface).

We next turn in Figure 13 to examine the results for one specific summer, namely 1999, to gain more insight into the different performance of the four cases. The summer of 1999 was suggested for our examination by CPC. The precipitation observations (Figure 14) indicate that the southwest U.S. monsoon was strong that year, with July precipitation well above normal in Arizona and western New Mexico. Additionally, the northern Midwest experienced well above normal July precipitation, while the lower Mississippi River basin experienced substantially below normal precipitation.

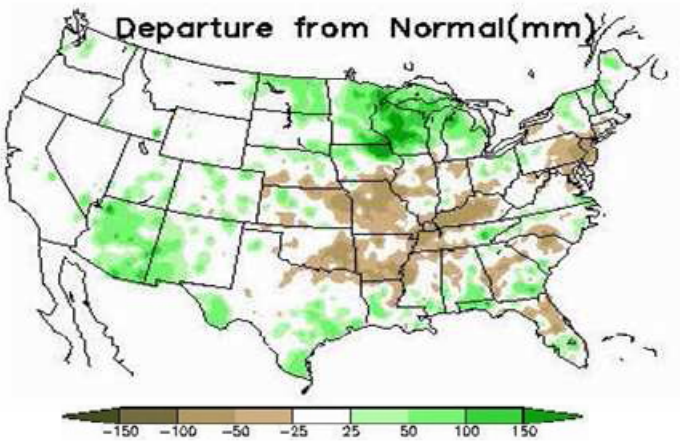

Figure 14 Observed precipitation anomaly of July 1999.

The four panels of Figure 13 show the CFS predicted precipitation anomaly of July 1999 for each Case A-D (wherein the anomaly depicted for each case is derived with respect to the CFS climatology of that case). Hence we are essentially looking for which CFS configurations can reproduce even the correct SIGN and SIGNGRADIENT of the observed precipitation anomaly. Thus, with respect to the sign of the anomaly, Figure 13 reveals that Case C (CFS with Noah LSM and GLDAS/Noah initial land states) indeed had the most consistently good performance among all four configurations.

Once again, Figure 13 shows how poorly Case B performed. This is the configuration where the CFS/Noah model configuration used GR2 initial land states. As indicated in Figures 1-8, the differences between the GR2/OSU and GLDAS/Noah initial land states indicates that both their climatology and spatial anomalies of soil moisture are quite different, with GLDAS/Noah having higher soil moisture values in the warm season over most non-arid regions worldwide, than that of GR2 with the OSU LSM from GR2.

Also noteworthy from Figure 13 is the degradation in Case D versus Case C, hence for July 1999 the CFS/Noah performance is worse if the climatology of GLDAS/Noah is used for initial land states in place of the instantaneous states of GLDAS/Noah.

Finally from Figure 13, the control Case A(with older OSU LSM and GR2 as source of initial land states) appears to yield somewhat better anomaly pattern in the southwest monsoon region, but clearly performs worse than Case C for the spatially large anomalies of the northern Midwest and lower Mississippi Valley.

3. Conclusions

The CFS experiments presented here demonstrate the positive impact from use of the Noah LSM and the GLDAS. Here are the main conclusions from these experiments.

- CFS prediction skill for CONUS summer season precipitation is marginally improved by the upgrade from OSU LSM to Noah LSM, provided that Noah-compatible initial land states are provided with properly spun-up land initial conditions (such as via a GLDAS executing the same Noah LSM).
- Even with improved prediction skill from combination of LSM upgrade and compatible GLDAS-generated initial conditions, the CONUS-average summer season prediction skill for precipitation remains low.
- A disturbingly inaccurate picture of the impact of an LSM upgrade can be obtained by not providing initial land states compatible with the new LSM.

- The climate model prediction skill was actually degraded by the new LSM if self-consistent initial land states were not provided.
- The use of initial soil moisture states with instantaneous soil moisture anomalies did not appear to provide a clear-cut advantage over climatological soil moisture states, provided the soil moisture climatology was produced by the same land model being tested in global forecast model.

4. Future works

We will execute and assess the corresponding winter season reforecasts of the new CFS over the same 25 years. To save computational resources, we will assess only Cases A and C.

For both the summer and winter reforecasts, we will expand our assessment of the CFS hindcasts experiments to include Asia, Europe and South America, plus assess other fields besides precipitation, such as near surface air temperature, large-scale height and circulation fields, and low-level jets. In particular, we will add assessment of the SST anomaly fields predicted by the four CFS cases to determine to what degree the changes in the land treatment effected the larger-scale global circulation patterns and hence the coupled SST prediction. A recent study [Schubert et al. 2004] has firmly established the important role of Pacific and Atlantic SST anomalies as substantial causes of significant warm-season drought over the CONUS. Additionally, we will focus on the CFS predictions of the 1988 major summer drought event and the 1993 major summer flood event, as well as the additional strong southwest U.S. monsoon event of summer of 1990.

Very importantly, we will enlist the CFS Assessment Team of the NOAA-NCEP Climate Test Bed to carry out their own independent evaluations of our CFS experiments.

Lastly, we will execute CFS impact tests for future Noah LSM upgrades not yet embodied in the Noah LSM version used in the CFS experiments here. Two anticipated Noah upgrades are a dynamic vegetation treatment and a multi-layer snowpack treatment. Noah currently employs a single bulk-layer treatment of the snowpack. Such CFS impact tests will require re-execution of the retrospective GLDAS/Noah in order to include the same Noah upgrades in GLDAS.

Acknowledgements. We would like to thank S. Saha, S. Moorthi, W. Wang, C. Thiaw and H. Wei for their helps during these experiments.

References

Dirmeyer, A. P., Dolman, A., and Sato, N. 1999. The Global Soil Wetness Project: A Pilot Project for Global Surface Modeling and Validation. *Bull. Amer. Meteor. Soc.*, **80**, 851–878.

Dirmeyer, A. P., Gao, X., Zhao, M., Guo, Z., Oki, T., and Hanasaki, N. 2006. GSWP-2: Multimodel Analysis and Implications for Our Perception of the Land Surface. *Bull. Amer. Meteor. Soc.*, **87**, 1381–1397.

Koster, R., Dirmeyer, P. A., Guo, Z., Bonan, G., Chan, E., Cox, P., Gordon, C. T., Kanae, S., Kowalczyk, E., Lawrence, D., Liu, P., Lu, C.-H., Malyshev, S., McAvaney, B., Mitchell, K., Mocko, D., Oki, T., Oleson, K., Pitman, A., Sud, Y. C., Taylor, C. M., Verseghy, D., Vasic, R., Xue, Y., and Yamada, T. 2004. Regions of Strong Coupling between Soil Moisture and Precipitation. *Science*, **305**, 1138–1140.

Koster, R. and Milly, C. 1997. The Interplay Between Transpiration and Runoff Formulations in Land Surface Schemes Used with Atmospheric Models. *J. Climate*, **10(7)**, 1578–1591.

Mitchell, K., Lohmann, D., Houser, P. R., Wood, E. F., Schaake, J. C., Robock, A., Cosgrove, B. A., Sheffield, J., Duan, Q., Luo, L., Higgins, R. W., Pinker, R. T., Tarpley, J. D., Lettenmaier, D. P., Marshall, C. H., Entin, J. K., Pan, M., Shi, W., Koren, V., Meng, J., Ramsay, B. H., and Bailey, A. A. 2004. The Multi-institution North American Land Data Assimilation System (NLDAS): Utilizing Mutiple GCIP Products and Partners in a Continental Distributed Hydrological Modeling System. *J. Geophys. Res.*, **109**, *D07S90*, DOI:10.1029/2003JD003823.

Rodell, M., Houser, P. R., Jambor, U., Gottschalck, J., Mitchell, K., Meng, C.-J., Arsenault, K., Cosgrove, B., Radakovich, J., Bosilovich, M., Entin, J. K., Walker, J. P., Lohmann, D., , and Toll, D. 2004. The Global Land Data Assimilation System. *Bull. Amer. Meteor. Soc.*, **85(3)**, 381–394.

Saha, S., Nadiga, S., Thiaw, C., Wang, J., Wang, W., Zhang, Q., van den Dool, H. M., Pan, H.-L., Moorthi, S., Behringer, D., Stokes, D., Pena, M., Lord, S., White, G., Ebisuzaki, W., Peng, P., and Xie, P. 2006. The NCEP Climate Forecast System. *J. Climate*, **19**, 3483–3517.

Schubert, S., Suarez, M., Pegion, P., Koster, R., and Bacmeister, J. 2004. Causes of Long-Term Drought in the U.S. Great Plains. *J. Climate*, **17**, 485–503.